Geometrically frustrated magnetic structures of the heavy-fermion compound CePdAl studied by powder neutron diffraction

1996 J. Phys.: Condens. Matter 8 11213

(http://iopscience.iop.org/0953-8984/8/50/043)

J. Phys.: Condens. Matter **8** (1996) 11213–11229. Printed in the UK

Geometrically frustrated magnetic structures of the heavy-fermion compound CePdAl studied by powder neutron diffraction

A Dönni†, G Ehlers‡, H Maletta‡, P Fischer†‖, H Kitazawa§ and M Zolliker†¶

† Laboratory for Neutron Scattering, ETH Zürich and Paul Scherrer Institute, CH-5232 Villigen PSI, Switzerland

‡ Hahn Meitner Institute Berlin, Glienicker Strasse 100, D-14092 Berlin, Germany

§ National Research Institute for Metals, Tsukuba, Ibaraki 305, Japan

Received 2 July 1996

Abstract. The heavy-fermion compound CePdAl with ZrNiAl-type crystal structure (hexagonal space group $P\bar{6}2m$) was investigated by powder neutron diffraction. The triangular coordination symmetry of magnetic Ce atoms on site 3f gives rise to geometrical frustration. CePdAl orders below $T_N = 2.7$ K with an incommensurate antiferromagnetic propagation vector $\boldsymbol{k} = [1/2, 0, \tau], \tau \approx 0.35$, and a longitudinal sine-wave (LSW) modulated spin arrangement. Magnetically ordered moments at Ce(1) and Ce(3) coexist with frustrated disordered moments at Ce(2). The experimentally determined magnetic structure is in agreement with group theoretical symmetry analysis considerations, calculated by the program MODY, which confirm that for Ce(2) an ordered magnetic moment parallel to the magnetically easy c-axis is forbidden by symmetry. Further low-temperature experiments give evidence for a second magnetic phase transition in CePdAl between 0.6 and 1.3 K. Magnetic structures of CePdAl are compared with those of the isostructural compound TbNiAl, where a non-zero ordered magnetic moment for the geometrically frustrated Tb(2) atoms is allowed by symmetry.

1. Introduction

Ternary rare-earth intermetallic compounds, in particular those containing Ce, are known to exhibit unusual magnetic properties at low temperatures, for example magnetic ordering in a heavy-fermion compound [1] and geometrical frustration in a triangular lattice with antiferromagnetic coupling [2, 3]. These two subjects coalesce with the recently discovered ternary intermetallic compound CePdAl [4–7]. On one hand CePdAl with hexagonal ZrNiAl-type crystal structure is an antiferromagnetically ordered ($T_N = 2.7$ K) heavy-fermion compound ($\gamma_0 = 270$ mJ mol^{-1} K^{-2}). On the other hand the triangular coordination symmetry of the magnetic Ce atoms gives rise to geometrical frustration. Both effects tend to shift the magnetic phase transition from the temperature corresponding to the exchange energy down to lower temperature. The resulting complex magnetic structures of CePdAl have been investigated in the present work.

‖ Author for further correspondence.

¶ Present address: Institute Laue–Langevin, BP 156, F-38042 Grenoble, France.

0953-8984/96/5011213+17$19.50

Magnetic properties reported for CePdAl are summarized in table 1. In CePdAl the enhanced γ_0-value, the low value of the magnetic entropy released at T_N, $S_{ord} = 0.38\ R \ln 2$, and the temperature dependence of electric resistivity [5, 6] give evidence for a pronounced Kondo effect with short-range Ce–Ce correlations above T_N. The hybridization strength between 4f and conduction electrons is stronger in CePdAl [5] than in CePtAl [5, 8] and, based on the observed pressure dependence of the specific heat anomaly [9], CePdAl seems to be located close to the maximum of T_N in Doniach's magnetic phase diagram.

Table 1. Magnetic properties reported for CePdAl with the hexagonal ZrNiAl-type crystal structure: a, c, room-temperature lattice parameters; T_N, Néel temperature; S_{ord}, magnetic entropy released at T_N; γ_0, electronic specific heat coefficient in the magnetically ordered state.

	Hulliger [4]	Schank *et al* [5]	Kitazawa *et al* [6]
a (Å)	7.2198(4)	7.219	7.2210(1)
c (Å)	4.2329(4)	4.231	4.2334(1)
c/a	0.586	0.586	0.586
T_N (K)	—	≈ 3	2.7(1)
S_{ord} ($R \ln 2$)	—	0.55	0.38
γ_0 (mJ mol^{-1} K^{-2})	—	250	270

Above 120 K the magnetic susceptibility of our CePdAl sample obeys a Curie–Weiss law. The effective magnetic moment of 2.53 μ_B is close to the free-ion value for Ce^{3+} of 2.54 μ_B and the paramagnetic Curie temperature $\Theta_p = -34$ K indicates antiferromagnetic interactions. The large value $|\Theta_p|/T_N = 12.6$ is a strong indicator of frustration in CePdAl.

The hexagonal ZrNiAl-type crystal structure (space group $P\bar{6}2m$) is an ordered derivative of the Fe_2P structure and consists of layers of Ce and Pd atoms, alternating along the c-direction with layers of Al and Pd. This crystal structure can be characterized as a high-temperature modification and is found for as-cast CePdAl samples, prepared by the standard arc-melting technique [5]. In the series of rare-earth palladium aluminides LnPdAl [7] the ZrNiAl-type high-temperature modification is adopted for as-cast samples of all rare-earth compounds (Ln = Ce, Pr, Nd, Sm, Gd, Tb, Dy, Ho, Er, Tm, Lu) except for LaPdAl (LaNiAl-type structure) and for YbPdAl (TiNiSi-type structure). After an annealing process at 750 °C the LnPdAl samples (Ln = Sm, Gd, Tb, Dy, Ho, Er, Tm, Yb, Lu) have transformed to a low-temperature modification with orthorhombic TiNiSi-type crystal structure (space group $Pnma$). Exceptions are PrPdAl and NdPdAl, which retain the ZrNiAl-type structure on annealing at 700 °C, and CePdAl, where an annealing process at temperatures between 700 and 900 °C causes a phase transition to an unknown crystal structure or possibly chemical decomposition.

Concurrently two independent powder neutron diffraction investigations on as-cast CePdAl samples have been carried out. One of these experiments has been performed at the Hahn–Meitner Institute (HMI) at Berlin, Germany. The other neutron diffraction study was done partly at reactor Saphir of the Paul Scherrer Institute (PSI) at Villigen, Switzerland, and partly at the Institute Laue–Langevin (ILL) at Grenoble, France. The results of the two experiments are presented in this paper together with group theoretical symmetry analysis considerations, calculated by the program MODY [10]. Experiment and theory both support the view that in CePdAl a geometrically frustrated magnetic structure with coexisting magnetically ordered Ce moments and disordered Ce moments is stable in a certain temperature range below $T_N = 2.7$ K. Magnetic structures of CePdAl are compared with those of the isostructural compound TbNiAl [3], where a non-zero ordered moment for the geometrically frustrated Tb atoms is allowed by symmetry.

2. Experimental details

Two different polycrystalline CePdAl samples were synthesized. One sample (CePdAl No 1) was prepared at HMI by inductive levitation melting of the pure elements under argon atmosphere. The elements had a purity of at least m4N. The resulting buttons were rather brittle. The other sample (CePdAl No 2) was synthesized in Japan by arc-melting the pure elements (Ce, 3N; Pd, 4N; Al, 5N) in an argon atmosphere under continuous titanium gettering. The sample was melted several times, turning it over each time. The average weight loss during melting was 0.4%. X-ray powder diffraction measurements using Cu Kα radiation confirmed for both as-cast CePdAl samples the presence of the ZrNiAl-type crystal structure with traces of impurity phase contributions restricted to below 1% of the observed x-ray Bragg intensities. After annealing part of the CePdAl material for 7 d at 850 °C (at HMI) and for 5 d at 900 °C (in Japan) the ZrNiAl-type crystal structure had disappeared. Thus, as-cast CePdAl powder samples were used to perform the neutron diffraction experiments.

The CePdAl sample No 1 (about 10 g) was investigated at HMI on the multicounter powder neutron diffractometer E6. The incident neutron wavelength of $\lambda = (2.437 \pm 0.001)$ Å was determined in advance using a YIG sample. Experiments down to 1.3 K were carried out by using a ^{4}He ILL standard orange cryostat and a cylindrical vanadium sample container. Low-temperature measurements were performed at 600 and 53 mK with $\lambda = (2.427 \pm 0.002)$ Å. About 5 g CePdAl material was enclosed into a cylindrical copper container and cooled in a ^{3}He–^{4}He dilution refrigerator. The CePdAl sample No 2 (about 16 g) was studied at reactor Saphir at PSI on the multicounter powder neutron diffractometer DMC [11], which is equipped with 400 detectors. The incident neutron wavelength $\lambda = (1.700 \pm 0.002)$ Å was obtained from a vertically focused germanium (3, 1, 1) monochromator. Diffraction patterns were recorded both in the high-resolution mode (HR, primary collimation $\alpha_1 = 10'$) at 7.5 K and in the high-intensity mode (HI, primary collimator removed) at 7.5 and 1.5 K. All intensities were corrected for absorption according to the measured transmission (μR = 0.126). To examine the temperature dependence of magnetic Bragg intensities down to 1.5 K additional neutron diffraction experiments on the CePdAl sample No 2 were carried out at ILL. The thermal triple-axis spectrometer IN3 was operated in the two-axis mode by using a neutron wavelength $\lambda = 2.36$ Å, a pyrolytic graphite filter and collimations of open and 30′ in front of and behind the sample, respectively.

3. Results and analysis

3.1. The crystal structure of CePdAl

The DMC (HR) neutron diffraction pattern of CePdAl (sample No 2) in its paramagnetic state at 7.5 K is displayed in figure 1. The observed intensity distribution corresponds to a ternary compound possessing the hexagonal ZrNiAl-type crystal structure (space group $P\bar{6}2m$ with Ce on the 3f sites, Pd on the 1a and 2d sites and Al on the 3g sites). A total of 66 inequivalent nuclear Bragg reflections in the scattering angle range $12^\circ \leqslant 2\Theta \leqslant 125^\circ$ were refined by the program FullProf [12], including a fit of the background represented by a self-adjusting polynomial. The resulting structural parameters for CePdAl at 7.5 K are listed in table 2. The refinement, based on the nuclear scattering lengths published by Sears [13], finally converged to the agreement values $R_{wp} = 5.16\%$ and $R_{I,N} = 3.64\%$, concerning weighted and integrated intensities, respectively. From counting statistics the expected value is calculated to be $R_{exp} = 2.62\%$, yielding $\chi^2 = (R_{wp}/R_{exp})^2 = 3.88$.

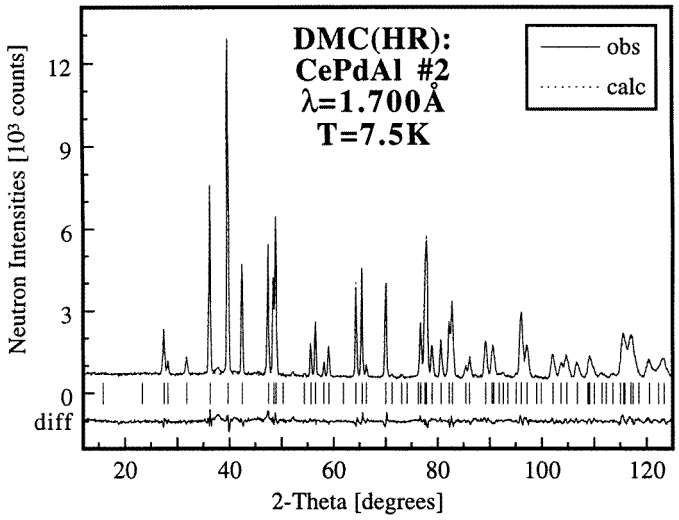

Figure 1. A FullProf refinement of the hexagonal ZrNiAl-type crystal structure of paramagnetic CePdAl at 7.5 K. Peak positions are indicated by vertical bars. The neutron powder diffraction pattern was recorded at PSI with a counting time of 5 h/point using the DMC high-resolution mode (sample No 2).

Table 2. Hexagonal ZrNiAl-type crystal structure parameters (space group $P\bar{6}2m$) of CePdAl at 7.5 K, refined from neutron powder diffraction data of sample No 2. The relative errors given in parentheses include estimated standard deviations of the fit and the error of the neutron wavelength calibration.

$a = 7.195(9)$ Å		$c = 4.240(5)$ Å		$c/a = 0.5893(1)$	
Atom	Site	x/a	y/b	z/c	B (Å^2)
Ce	3f	0.5785(4)	0	0	0.35(6)
Pd	1a	0	0	0	0.28(7)
Pd	2d	1/3	2/3	1/2	0.26(6)
Al	3g	0.2280(5)	0	1/2	0.38(8)

The crystal structure of CePdAl is shown in figure 2(a) as a view onto the hexagonal a–b-plane. The crystallographic unit cell contains three magnetic Ce atoms with positions Ce(1) at $(0.58, 0, 0)$, Ce(2) at $(0, 0.58, 0)$ and Ce(3) at $(0.42, 0.42, 0)$. Concerning interatomic Ce–Ce distances at 7.5 K, Ce(1) has four nearest neighbours Ce(2) and Ce(3) at 3.73 Å and two second-nearest neighbours Ce(1) at 4.24 Å. Nearest neighbours form triangular lattices inside a–b-planes, whereas second-nearest neighbours form chains parallel to the c-axis.

According to the neutron diffraction patterns of samples No 1 and No 2 the hexagonal ZrNiAl-type crystal structure remains stable upon cooling a CePdAl as-cast sample from room temperature down to 53 mK. The thermal expansion of CePdAl is anisotropic with the ratio of lattice constants c/a increasing from 0.586 at room temperature to 0.589 at 1.3 K and with the Ce–Ce nearest-neighbour distance decreasing from 3.74 Å at room temperature [14] to 3.73 Å at 7.5 K.

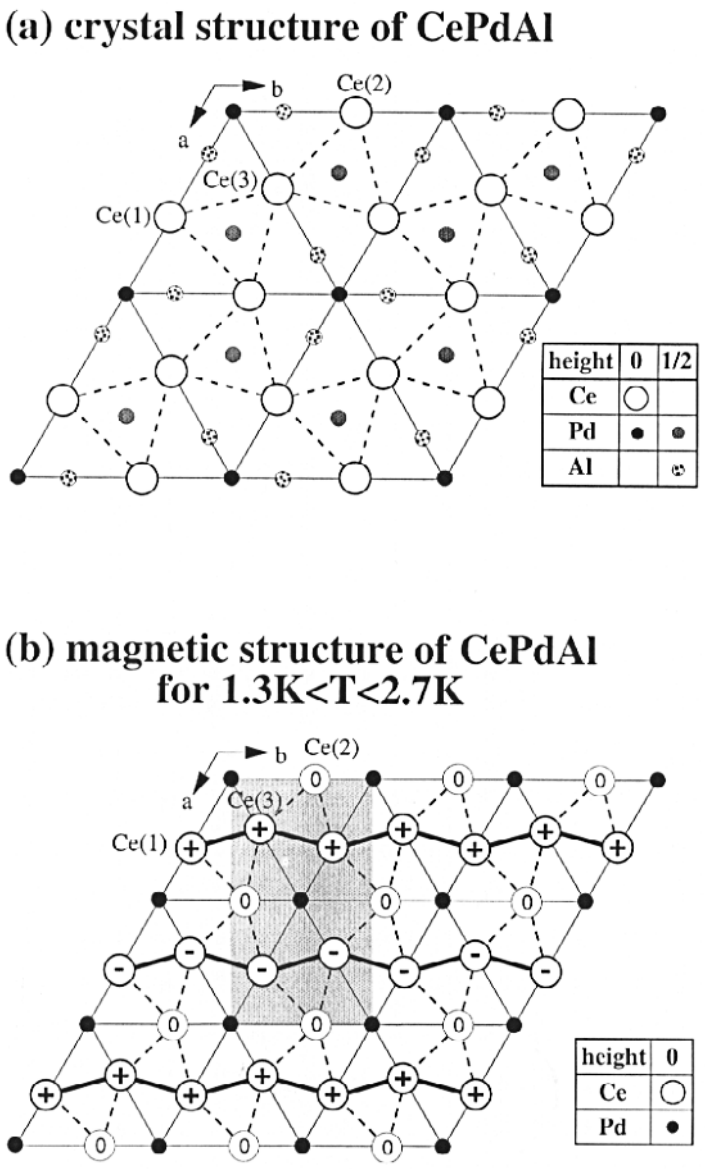

Figure 2. (a) The crystal structure of CePdAl (ZrNiAl type) plotted as a view onto the hexagonal a–b plane. The heights of the atoms are in units of (z/c). Dashed lines illustrate the triangular lattice of the magnetic Ce atoms. (b) The basal plane of the magnetic structure of CePdAl for 1.3 K$< T <$ 2.7 K. The magnetic Ce moments are partly ordered (parallel (+) and antiparallel (−) to the c-axis) and partly disordered (0). The unit cell for the orthorhombic description of the crystal structure is highlighted by the grey colour.

3.2. The magnetic structure of CePdAl at 1.5 K

The neutron diffraction patterns of CePdAl recorded at 1.5 K for sample No 2 (see figure 3) and at 1.3 K for sample No 1 (see figure 4) contain weak additional Bragg peaks which arise from scattering on ordered magnetic moments of Ce atoms. Magnetic lines of CePdAl can

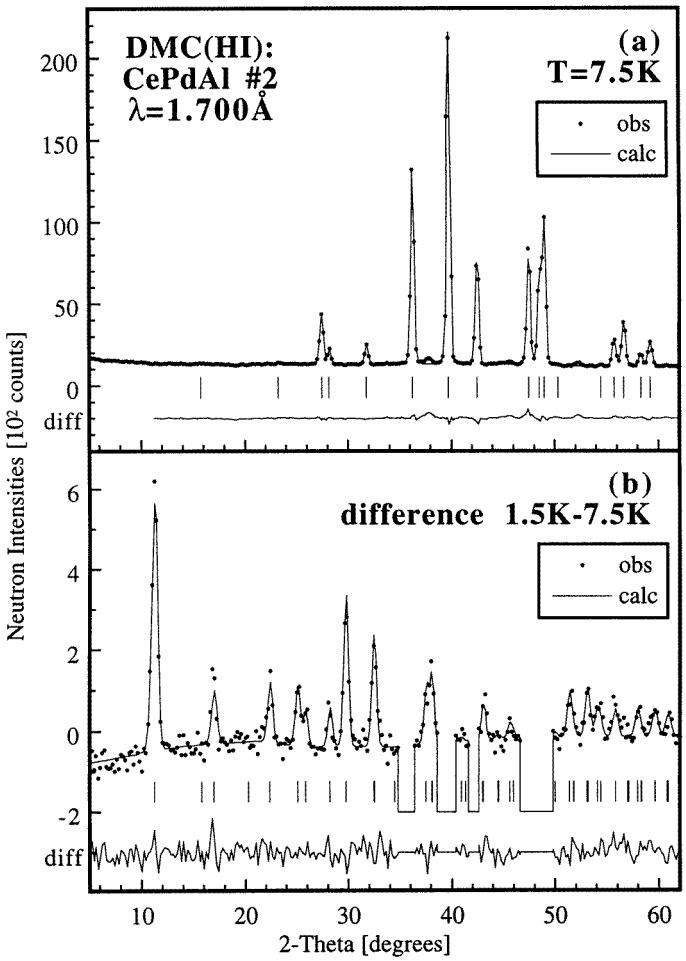

Figure 3. FullProf refinements of (a) the crystal structure of CePdAl at 7.5 K and (b) the magnetic structure of CePdAl at 1.5 K (obtained from the difference pattern 1.5 K − 7.5 K). Peak positions are indicated by vertical bars. The neutron powder diffraction patterns at 1.5 and 7.5 K were recorded at PSI with a counting time of 21 h/point using the DMC high-intensity mode (sample No 2). The difference pattern (b) exhibits a negative background level for small 2Θ values, which reflects the change of background between the paramagnetic and magnetically ordered phase of CePdAl. Data points with 2Θ values near intense nuclear Bragg peaks were excluded from the refinement of the difference pattern (b) because of large error bars.

all be indexed by an incommensurate antiferromagnetic propagation vector $\boldsymbol{k} = [1/2, 0, \tau]$ with $\tau \approx 0.35$. As shown in figure 3(b) the strongest magnetic intensity appears for the peak $(1/2, 0, \tau)$ at $2\Theta = 11.2^\circ$, whereas no magnetic intensity is observed for the reflections $(-1/2, 1, -\tau)$ at $2\Theta = 15.8^\circ$ and $(-1/2, 1, 1-\tau)$ at $2\Theta = 20.3^\circ$.

For the CePdAl sample No 2 the magnetic structure at 1.5 K was determined by FullProf refinements from the DMC(HI) pattern at 7.5 K (only the nuclear contribution; see figure 3(a) and from the difference pattern 1.5 K − 7.5 K (only the magnetic contribution, see figure 3(b)). To reduce the number of free parameters, backgrounds were described by interpolating between several selected points. For the fit of the nuclear contribution

(figure 3(a)) the structural parameters of table 2 were kept fixed and the values of the resolution parameters (pseudo-Voigt peak shape), the scale factor and the zero point of the diffractometer were refined. For the fit of the magnetic contribution (figure 3(b)) the only free parameters were components of the ordered magnetic Ce moments, the component τ of the propagation vector and one factor scaling the resolution parameters. The latter was necessary to correct for the experimental fact that the width of magnetic reflections appeared to be broader than for nuclear reflections, indicating smaller magnetic domain sizes. Table 3 contains the magnetic structure data for CePdAl at 1.5 K derived by FullProf profile analysis of 46 inequivalent magnetic peaks (figure 3(b)) with agreement values $R_{wp} = 9.03\%$, $R_{I,M} = 10.3\%$, $R_{exp} = 7.38\%$ and $\chi^2 = 1.50$.

For the CePdAl sample No 1, crystal and magnetic structures were simultaneously analysed by the FullProf program from the E6 pattern measured at 1.3 K (see figure 4). A refinement of six inequivalent nuclear Bragg peaks and 13 inequivalent magnetic Bragg peaks in the scattering angle range $13^\circ \leqslant 2\Theta \leqslant 54.5^\circ$ yielded the best fit ($\chi^2 = 2.70$) for the results listed in table 3.

Table 3. The magnetic structure of CePdAl at 1.3 and 1.5 K refined from neutron powder diffraction data of samples No 1 and No 2.

	x/a	y/b	z/c	μ_x	μ_y	μ_z
Ce(1)	0.58	0	0	0	0	μ_1
Ce(2)	0	0.58	0	0	0	0
Ce(3)	0.42	0.42	0	0	0	μ_1
Magnetic propagation vector $\boldsymbol{k} = [1/2, 0, \tau]$						
	1.3 K No 1	1.5 K No 2				
a (Å)	7.209(1)	7.195(9)				
c (Å)	4.243(1)	4.240(5)				
c/a	0.589	0.589				
Component τ	0.355(1)	0.350(1)				
Magnitude μ_1 (μ_B)	1.58(6)	1.58(2)				

Powder neutron diffraction experiments on two different CePdAl samples both favour an incommensurate antiferromagnetic structure with an LSW modulated spin arrangement as given in table 3. The two refinements yield similar values for the maximum amplitude $\mu_1 = (1.58 \pm 0.02)\ \mu_B$. The small difference obtained for the component τ might be caused by the different fit procedures (different numbers of Bragg reflections) or possibly hint at a sample dependence of the magnetic propagation vector. The accuracy of the structure determination is limited by the weakness of the observed magnetic powder neutron Bragg peaks. Within the precision of the measurements of figures 3 and 4 the agreement of the refined magnetic structure is excellent.

The magnetic structure of CePdAl at 1.5 K is illustrated in figure 2(b). Magnetically ordered moments at Ce(1) and Ce(3) coexist with disordered moments at Ce(2). The ordered magnetic Ce moments are oriented perpendicular to the basal plane and form ferromagnetic chains parallel to the b-axis with an antiferromagnetic coupling $+ - +-$ along the a-axis. The amplitude is constant for all atoms at a fixed height (z/c) and varies along the hexagonal c-axis according to the incommensurate component τ of the propagation vector. The disordered magnetic Ce(2) atoms, which are located between two ferromagnetic chains,

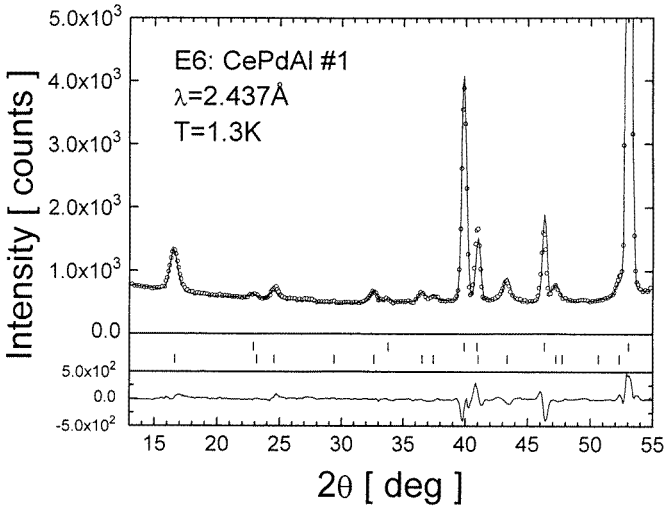

Figure 4. A FullProf refinement of the crystal and magnetic structures of CePdAl at 1.3 K. The upper row of vertical bars indicates the positions of nuclear reflections and the lower row those of the magnetic reflections. The neutron powder diffraction pattern was recorded at HMI using the diffractometer E6 (sample No 1).

are geometrically frustrated since they belong at the same time to a first triangle with two Ce nearest neighbours '+' and to a second triangle with two Ce nearest neighbours '−'.

As illustrated in figure 5 the magnetic Bragg peaks $(1/2, -2, \tau)$ and $(1/2, -2, 1-\tau)$ appear to be significantly broader than the nuclear Bragg peaks $(1, 1, 0)$, $(1, 0, 1)$ and $(2, 0, 0)$. The latter correspond well to the instrumental resolution of the E6 diffractometer. Based on the observed width of the $(1/2, -2, \tau)$ reflection (see figure 5) the correlation length of the incommensurate magnetic structure of CePdAl at 1.3 K can be estimated to be about 100 Å, which corresponds to a distance of 24 hexagonal unit cells along the c-axis.

3.3. Symmetry analysis

We now proceed to explain the determination of the magnetic structure of CePdAl (results of table 3) in more detail. Group theoretical calculations known as the symmetry analysis method allow us to find all models of magnetic structures that are compatible with the symmetry of the paramagnetic phase [10]. The magnetic representation $\boldsymbol{S}(\boldsymbol{r})$ is an axial vector function which can be presented as a direct sum of irreducible representations $\psi_\lambda^{\nu n}$ of the paramagnetic symmetry group G:

$$S(r) = \sum_{\nu\lambda n} c_\lambda^{\nu n} \psi_\lambda^{\nu n} \tag{1}$$

(ν, λ and n number the representation, its dimension and arms of the propagation vector $\boldsymbol{k}$, respectively). The coefficients $c_\lambda^{\nu n}$ form the order parameter of the phase transition.

For the case of CePdAl, which corresponds to a crystal structure with space group $P\bar{6}2m$ (Schoenflies symbol D_{3h}^3) and magnetic atoms on site 3f, the incommensurate magnetic propagation vector $\boldsymbol{k} = [1/2, 0, \tau]$ belongs to a star with six arms: $\boldsymbol{k}_1 = [1/2, 0, \tau]$, $\boldsymbol{k}_2 = -\boldsymbol{k}_1$, $\boldsymbol{k}_3 = [0, 1/2, \tau]$, $\boldsymbol{k}_4 = -\boldsymbol{k}_3$, $\boldsymbol{k}_5 = [1/2, 1/2, \tau]$ and $\boldsymbol{k}_6 = -\boldsymbol{k}_5$. A calculation by the program MODY [10] performed for $\boldsymbol{k}_1$ and $\boldsymbol{k}_2$ gives the possible magnetic modes listed in table 4.

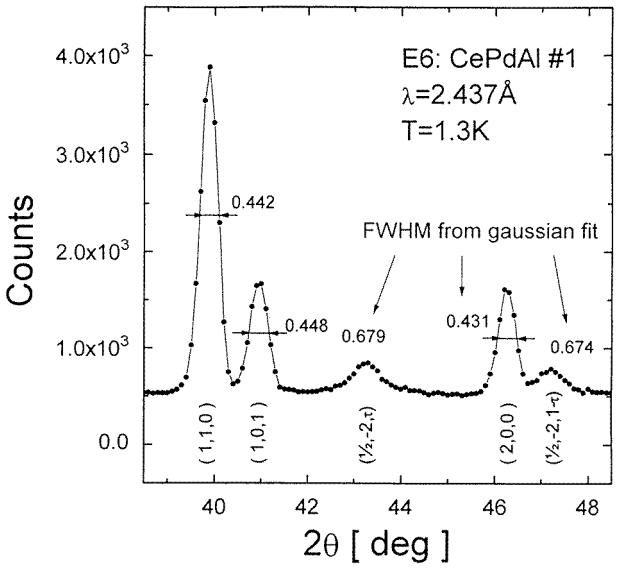

Figure 5. The E6 neutron diffraction pattern of CePdAl at 1.3 K (sample No 1) illustrating the different widths of nuclear and magnetic Bragg peaks.

The magnetic Ce atoms on site 3f are split into two independent types, called orbits in [10], with positions $(0.58, 0, 0)$ and $(0.42, 0.42, 0)$ belonging to type 1 and position $(0, 0.58, 0)$ to type 2. The magnetic propagation vector $\boldsymbol{k} = [1/2, 0, \tau]$ can be considered as a superposition $\boldsymbol{k} = \boldsymbol{k}_c + \boldsymbol{k}_{ic}$ of a commensurate antiferromagnetic component $\boldsymbol{k}_c = [1/2, 0, 0]$ inside the basal plane and an incommensurate component $\boldsymbol{k}_{ic} = [0, 0, \tau]$ along the hexagonal c-direction. The component $\boldsymbol{k}_c$ causes a lowering of symmetry at the magnetic phase transition from hexagonal for the crystal structure (space group $P\bar{6}2m$, No 189) to orthorhombic for the magnetic structure (space group $Amm2$, No 38, with $a_{\text{ortho}} = c_{\text{hex}}$; $b_{\text{ortho}} = \sqrt{3}a_{\text{hex}}$; $c_{\text{ortho}} = a_{\text{hex}}$). A change of the description of the CePdAl crystal structure from hexagonal to orthorhombic implies for the magnetic Ce atom a transformation from the hexagonal site

Ce	(3f)	$(x, 0, 0)$	$x = x_0$	$(P\bar{6}2m)$

to two inequivalent orthorhombic sites

Ce	(4d)	$(0, y, y)$	$y = (1 - x_0)/2$	$(Amm2)$
Ce	(2a)	$(0, 0, z)$	$z = x_0$	$(Amm2)$

which correspond to types 1 and 2, respectively. However, because of the incommensurate component $\boldsymbol{k}_{ic}$ no finite magnetic unit cell exists and the magnetic structure of CePdAl may be described either by the hexagonal unit cell and the propagation vector $\boldsymbol{k}_1 = [1/2, 0, \tau]$ (used in table 3) or by the orthorhombic magnetic unit cell marked by the grey colour in figure 2(b) and a propagation vector $\boldsymbol{k}_{\text{ortho}} = [\tau, 0, 0]$.

The magnetic wave vector group G_k decomposes into two one-dimensional irreducible representations τ_1 and τ_2 which both appear three times in type 1 and appear once and twice, respectively, in type 2. With respect to the two generators of the group G_k, $\{1\}$ (identity) and $\{m(0, y, z)\}$ (mirror plane $(0, y, z)$), the representations τ_1 and τ_2 have characters $(+, +)$ and $(+, -)$, respectively.

Table 4. Magnetic modes calculated by the program MODY [10] for the case of space group $P\bar{6}2m$, site 3f and incommensurate propagation vectors $\boldsymbol{k}_1 = [1/2, 0, \tau]$, $\boldsymbol{k}_2 = -\boldsymbol{k}_1$.

			(0.58, 0, 0)			(0, 0.58, 0)			(0.42, 0.42, 0)		
			x	y	z	x	y	z	x	y	z
Representation τ_1 $(+,+)$											
$\boldsymbol{k}_1$	type 1	${}^1\psi^{11\prime}$	1	0	0				−1	−1	0
		${}^1\psi^{11\prime\prime}$	0	1	0				0	1	0
		${}^1\psi^{11\prime\prime\prime}$	0	0	1				0	0	1
$\boldsymbol{k}_1$	type 2	${}^2\psi^{11\prime}$				1	0.5	0			
$\boldsymbol{k}_2$	type 1	${}^1\psi^{12\prime}$	1	0	0				−1	−1	0
		${}^1\psi^{12\prime\prime}$	0	1	0				0	1	0
		${}^1\psi^{12\prime\prime\prime}$	0	0	1				0	0	1
$\boldsymbol{k}_2$	type 2	${}^2\psi^{12\prime}$				1	0.5	0			
Representation τ_2 $(+,-)$											
$\boldsymbol{k}_1$	type 1	${}^1\psi^{21\prime}$	1	0	0				1	1	0
		${}^1\psi^{21\prime\prime}$	0	1	0				0	−1	0
		${}^1\psi^{21\prime\prime\prime}$	0	0	1				0	0	−1
$\boldsymbol{k}_1$	type 2	${}^2\psi^{21\prime}$				0	1	0			
		${}^2\psi^{21\prime\prime}$				0	0	1			
$\boldsymbol{k}_2$	type 1	${}^1\psi^{22\prime}$	1	0	0				1	1	0
		${}^1\psi^{22\prime\prime}$	0	1	0				0	−1	0
		${}^1\psi^{22\prime\prime\prime}$	0	0	1				0	0	−1
$\boldsymbol{k}_2$	type 2	${}^2\psi^{22\prime}$				0	1	0			
		${}^2\psi^{22\prime\prime}$				0	0	1			

The function $\boldsymbol{S}(\boldsymbol{r})$ must be real. Thus, in the case of an incommensurate propagation vector $\boldsymbol{k}$ it has to be described by irreducible representations $\psi_\lambda^{\nu n}$ belonging to the two arms $\boldsymbol{k}_1$ and $\boldsymbol{k}_2 = -\boldsymbol{k}_1$. The magnetic structure given in table 3 belongs to the representation τ_1 and corresponds to the mode

$$\boldsymbol{S}(\boldsymbol{r}) = C\,{}^1\psi^{11\prime\prime\prime} + C^*\,{}^1\psi^{12\prime\prime\prime} \tag{2}$$

with the order parameter

$$p = (C, C^*) = (\mu_1/2\exp(\mathrm{i}\alpha), \mu_1/2\exp(-\mathrm{i}\alpha)). \tag{3}$$

Including the hexagonal lattice translation vector $\boldsymbol{t}_n$, the corresponding magnetic Ce moments of the 3f sites are parallel or antiparallel to the hexagonal c-axis:

$$\begin{aligned}
&\text{Ce(1)} \qquad \boldsymbol{S}_{1n} = \boldsymbol{S}(\boldsymbol{r}_1 + \boldsymbol{t}_n) = \mu_1 \cos(\alpha + \boldsymbol{k}_1 \cdot \boldsymbol{t}_n) \cdot \boldsymbol{e}z \\
&\text{Ce(2)} \qquad \boldsymbol{S}_{2n} = \boldsymbol{S}(\boldsymbol{r}_2 + \boldsymbol{t}_n) = 0 \\
&\text{Ce(3)} \qquad \boldsymbol{S}_{3n} = \boldsymbol{S}(\boldsymbol{r}_3 + \boldsymbol{t}_n) = \mu_1 \cos(\alpha + \boldsymbol{k}_1 \cdot \boldsymbol{t}_n) \cdot \boldsymbol{e}z.
\end{aligned} \tag{4}$$

In table 3 the arbitrary phase factor is chosen as $\alpha = 0$. The symmetry of the magnetic structure (4) gives rise to a set of forbidden magnetic reflections $(-h/2, h, k \pm \tau)$ and any non-zero ordered magnetic moment at the frustrated atoms Ce(2) implies a violation of this extinction rule. In the neutron difference pattern of figure 3(b) no intensity can be detected for the forbidden reflections $(-1/2, 1, -\tau)$ at $2\Theta = 15.9^\circ$ and $(-1/2, 1, 1-\tau)$ at $2\Theta = 20.4^\circ$.

In general many symmetry-allowed magnetic structures are possible for CePdAl. They correspond to linear combinations of irreducible representations $\psi_\lambda^{\nu n}$ of table 4. Among them only two magnetic structures are compatible with the extinction rule $(-h/2, h, k \pm \tau)$.

One is the LSW modulated structure given by (2) with the ordered moments perpendicular to the basal plane. The other is a transverse sine-wave (TSW) modulated structure described by

$$\boldsymbol{S}(\boldsymbol{r}) = C\,{}^{1}\psi^{11''} + C^{*}\,{}^{1}\psi^{12''} \tag{5}$$

with ordered moments inside the basal plane. The structures (2) and (5) both belong to the representation τ_1. FullProf refinements clearly favour the LSW structure (result of table 3) with $\chi^2 = 1.50$ against the TSW structure (5) with $\chi^2 = 7.05$.

A very recent magnetization experiment on a CePdAl single crystal [15] revealed at 1.6 K highly anisotropic values of 1.38 μ_B/Ce and 0.11 μ_B/Ce for an external field of 7 T applied parallel and perpendicular to the hexagonal c-axis, respectively. In CePdAl the presence of a pronounced magnetic anisotropy fixes the direction of the ordered Ce moments to be perpendicular to the basal plane as deduced from neutron diffraction data. However, the symmetry of the representation τ_1 (table 4) does not allow a solution with the frustrated Ce(2) moments pointing along the magnetically easy c-direction. Therefore, an ordered moment at the Ce(2) position can only appear if either the magnetic anisotropy or the symmetry of the representation τ_1 is broken. In this sense symmetry analysis considerations can rationalize that in CePdAl a geometrically frustrated magnetic structure with coexisting ordered and disordered moments is stable in a certain temperature range below $T_N = 2.7$ K.

3.4. The temperature dependence of the magnetic Bragg intensities

The temperature dependence of powder neutron intensities of selected magnetic and nuclear Bragg peaks of CePdAl (sample No 2) was studied between 1.5 and 7.5 K. Scans through the forbidden magnetic reflections $(-1/2, 1, -\tau)$ and $(-1/2, 1, 1-\tau)$ failed to detect magnetic intensity and confirmed the validity of the extinction rule $(-h/2, h, k \pm \tau)$ down to 1.5 K. Figure 6 displays 2Θ scans through the strongest magnetic peak $(1/2, 0, \tau)$ measured at 1.50, 2.46 and 3.0 K. The gain of magnetic Bragg intensity upon cooling is connected with a clear shift of the peak position towards smaller 2Θ values. The latter gives rise to a change of the incommensurate component τ of the propagation vector $\boldsymbol{k} = [1/2, 0, \tau]$ as shown in figure 7(b). The temperature dependence of the integrated intensity of the $(1/2, 0, \tau)$ Bragg peak describes a second-order phase transition with a Néel temperature $T_N = (2.8 \pm 0.1)$ K, which is compatible with the specific heat anomaly [5] (see figure 7(a)).

In CePdAl the amount of magnetic entropy released below 1.5 K cannot be neglected. Figure 8 displays the low angle part of neutron diffraction patterns of CePdAl (sample No 1) measured at 1.3 K ($\lambda = 2.437$ Å) and at 600 and 53 mK ($\lambda = 2.427$ Å). Compared to the 1.3 K data measured with the ^{4}He cryostat the two low-temperature patterns measured with the dilution cryostat suffer from a poor signal-to-background ratio. For the nuclear Bragg peak $(1, 1, 0)$ (see figure 4 at $2\Theta = 39.9^\circ$), the ratio I_{max} to background is reduced from 6.2 ± 0.1 at 1.3 K to 1.01 ± 0.01 at 600 mK. Similar to the case for the strongest magnetic Bragg peak $(1/2, 0, \tau)$, the ratio I_{max} to background decreases from 0.9 ± 0.1 at 1.3 K to only 0.09 ± 0.01 at 600 mK. The poor quality of the dilution patterns does not allow a reliable determination of the magnetic structure of CePdAl at 600 and 53 mK. Nevertheless the spectra of figure 8 give evidence for a second magnetic phase transition in CePdAl at 600 mK $< T_{N,2} <$ 1.3 K. Magnetic Bragg peaks at 600 mK can be partly indexed with a similar incommensurate propagation vector $\boldsymbol{k} = [1/2, 0, \tau]$, $\tau = 0.350 \pm 0.005$, but magnetic intensities change essentially between 1.3 K and 600 mK (see figure 8). The two dilution patterns contain additional weak peaks (not clearly visible in figure 8) which suggest the presence of a second inequivalent magnetic propagation vector in CePdAl.

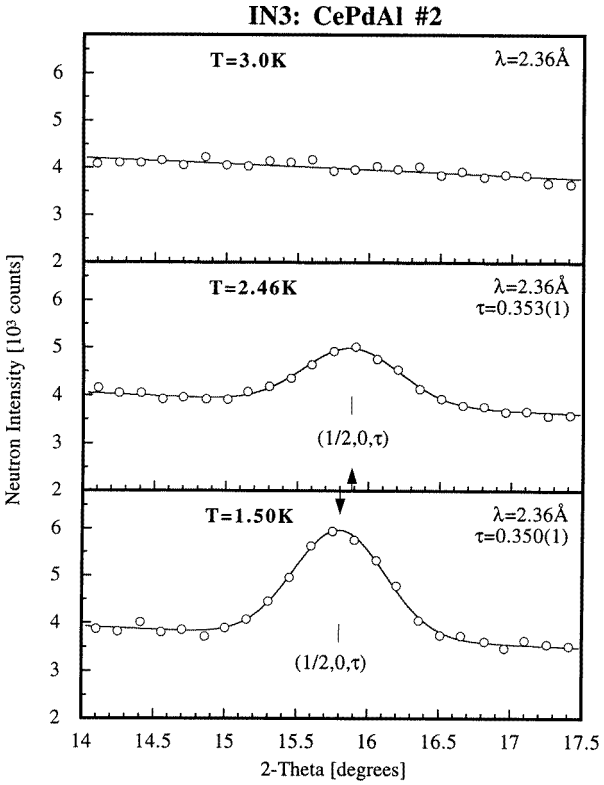

Figure 6. 2Θ scans through the strongest incommensurate magnetic peak $(1/2, 0, \tau)$ of CePdAl, measured at different temperatures (sample No 2).

4. Discussion

It is interesting to compare the effects of geometrical frustration on the magnetic structures of the isostructural compounds CePdAl and TbNiAl (see table 5). A powder neutron diffraction study [3] on TbNiAl revealed two magnetic phase transitions at $T_{N,1} = 47$ K and at $T_{N,2} = 23$ K. Antiferromagnetic structures of TbNiAl are illustrated in figures 9(a) (23 K $< T <$ 47 K) and (b) (2 K $< T <$ 23 K). Within experimental uncertainty all ordered Tb moments are determined to be parallel or antiparallel to the hexagonal c-axis, which suggests a similar magnetic anisotropy for the two compounds, TbNiAl and CePdAl. Table 6 contains the possible magnetic modes calculated by the program MODY [10] for the case of TbNiAl (space group $P\bar{6}2m$, magnetic Tb atoms on site 3f and a propagation vector $\boldsymbol{k}_1 = [1/2, 0, 1/2]$). The commensurate antiferromagnetic propagation vector $\boldsymbol{k}_1$ belongs to a star of three arms: $\boldsymbol{k}_1 = [1/2, 0, 1/2]$, $\boldsymbol{k}_2 = [0, 1/2, 1/2]$ and $\boldsymbol{k}_3 = [1/2, 1/2, 1/2]$. To facilitate the comparison with CePdAl the magnetic structures of TbNiAl are described with $\boldsymbol{k}_1$ and $\boldsymbol{k}_2$ (see table 5 and figure 9), differing from the equivalent description with $\boldsymbol{k}_3$ and $\boldsymbol{k}_2$ used in [3]. Similar to the case of CePdAl, the magnetic Tb atoms are split into two independent types with positions $(0.58, 0, 0)$ and $(0.42, 0.42, 0)$ belonging to type 1 and position $(0, 0.58, 0)$ to type 2 (see table 6). The magnetic wave vector group G_k decomposes into four one-dimensional irreducible representations τ_1, τ_2, τ_3 and τ_4, which appear in type 1 once, twice, once and twice, respectively, and in type 2 not at all, once,

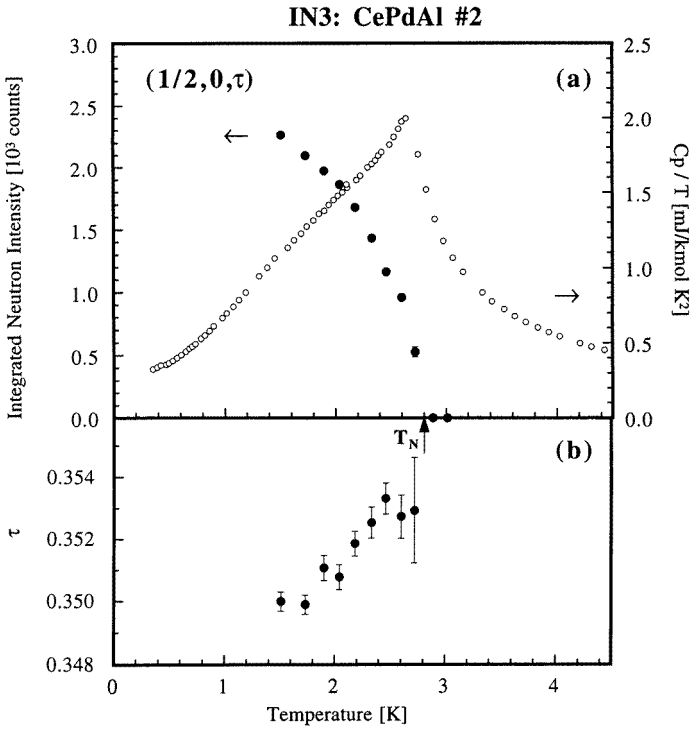

Figure 7. (a) The temperature dependence of the integrated neutron intensity of the strongest magnetic peak $(1/2, 0, \tau)$ of CePdAl (sample No 2) compared with the specific heat divided by temperature (C_p/T) from [5]. (b) The temperature dependence of the incommensurate component τ of the magnetic propagation vector $\boldsymbol{k} = [1/2, 0, \tau]$ based on the peak position of the $(1/2, 0, \tau)$ reflection.

once and once, respectively (see table 6). With respect to the four generators of the group $G_{\boldsymbol{k}}$, $\{1\}$ (identity), $\{m(0, y, z)\}$ (mirror plane $(0, y, z)$), $\{m(x, y, 0)\}$ (mirror plane $(x, y, 0)$) and $\{2(0, y, 0)\}$ (twofold axis $[0, y, 0]$), the representations τ_1, τ_2, τ_3 and τ_4 have characters $(+, +, +, +)$, $(+, -, -, +)$, $(+, -, +, -)$ and $(+, +, -, -)$, respectively. Between $T_{N,2}$ and $T_{N,1}$ the magnetic structure of TbNiAl shown in figure 9(a) belongs to the representation τ_3 and corresponds to the mode

$$\boldsymbol{S}(\boldsymbol{r}) = C_1\,{}^1\phi^{3'} + C_2\,{}^2\phi^{3'} \tag{6}$$

with the order parameter

$$p = (C_1, C_2) = (\mu_1, \mu_2). \tag{7}$$

A comparison of the magnetic structures of CePdAl (1.3 K $< T <$ 2.7 K) shown in figure 2(b) and TbNiAl (23 K $< T <$ 47 K) shown in figure 9(a) reveals that the chains parallel to the hexagonal b-axis are ferromagnetic for CePdAl (coupling between Ce(1) and Ce(3)) and antiferromagnetic for TbNiAl (coupling between Tb(1) and Tb(3)). The atoms Ce(2) and Tb(2) are both geometrically frustrated and a non-zero ordered magnetic moment parallel to the magnetically easy c-direction is forbidden by the symmetry of the magnetic structure of CePdAl (see representation τ_1 in table 3), in contrast to the symmetry of the magnetic structure of TbNiAl (see representation τ_3 in table 6) which allows such a component. In TbNiAl at 28 K the moment $\mu_2 = (1.2 \pm 0.3)\ \mu_B$ of the frustrated Tb(2)

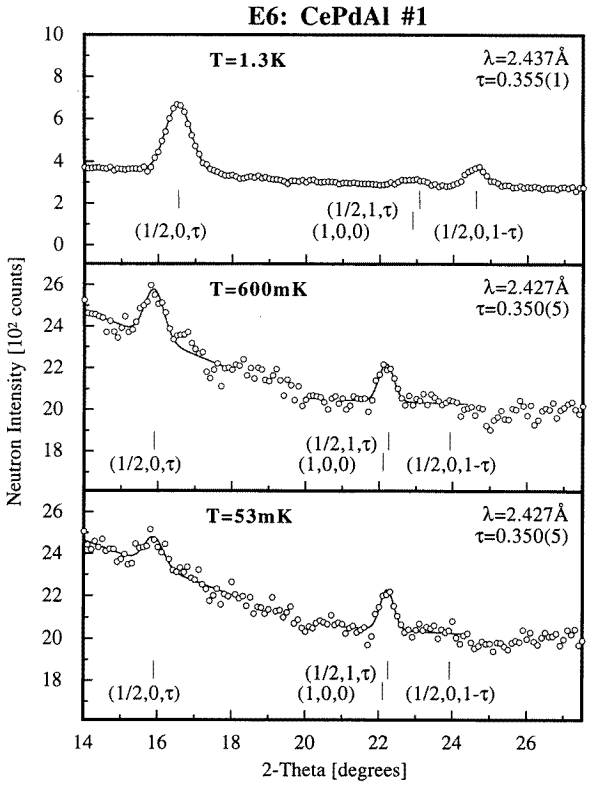

Figure 8. The low-angle part of neutron diffraction patterns of CePdAl (sample No 1) measured at 1.3 K ($\lambda = 2.437$ Å) and at 600 and 53 mK ($\lambda = 2.427$ Å). The spectra are calibrated to equal integrated neutron intensities of the nuclear Bragg peak (1, 1, 0).

atoms is strongly reduced below the value $\mu_1 = (7.9 \pm 0.2)\ \mu_B$ of Tb(1) and Tb(3) (see table 5).

For decreasing temperature TbNiAl shows a second magnetic phase transition at $T_{N,2} = 23$ K below which on one hand the value of μ_2 rapidly increases until it reaches $\mu_2 \approx \mu_1 = (8.7 \pm 0.1)\ \mu_B$ at 2 K and on the other hand the symmetry of the representation τ_3 is broken (a new propagation vector $\boldsymbol{k}_2 = [0, 1/2, 0]$ appears for Tb(2)). The low-temperature magnetic structure ($T < T_{N,2}$) of CePdAl is left to be determined in a future single-crystal neutron diffraction experiment. We expect that for the frustrated Ce(2) atom a non-zero ordered moment appears, which is fixed by the strong magnetic anisotropy to be perpendicular to the basal plane and which therefore implies a violation of the symmetry of the magnetic representation τ_1. However, the magnetic structure of CePdAl remains incommensurate down to 53 mK in contrast to the commensurate magnetic structure found in TbNiAl.

A common feature in the series of the isostructural hexagonal compounds LnNiAl (Ln = Tb, Dy, Ho) [3, 16] is the existence of at least two magnetic phase transitions at T_1 and T_2, which scale by $T_2 : T_1 \approx 1 : 2$. Geometrically frustrated magnetic Ln(2) moments appear with reduced values for $T_2 < T < T_1$ and change the magnetic propagation vector for $T < T_2$.

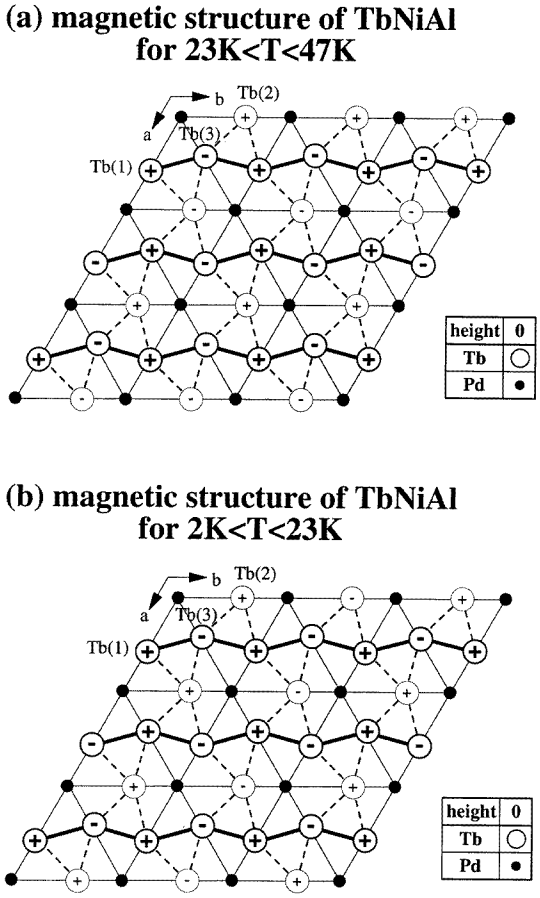

Figure 9. The basal plane of the magnetic structures determined for TbNiAl [3] (a) for 23 K $< T <$ 47 K and (b) for 2 K $< T <$ 23 K. Ordered magnetic Tb moments are parallel (+) or antiparallel (−) to the hexagonal c-axis.

5. Summary

Geometrically frustrated magnetic structures of the hexagonal heavy-fermion compound CePdAl with a triangular coordination symmetry of magnetic Ce atoms have been studied by means of powder neutron diffraction measurements. Below $T_N = 2.7$ K long-range magnetic order is found to be characterized by an incommensurate antiferromagnetic propagation vector $\boldsymbol{k} = [1/2, 0, \tau]$, $\tau \approx 0.35$, and an LSW modulated spin arrangement oriented along the hexagonal c-direction. Magnetically ordered moments at Ce(1) and Ce(3) coexist with frustrated disordered moments at Ce(2). Group theoretical symmetry analysis considerations, calculated by the program MODY, confirm that for the frustrated Ce(2) atoms an ordered magnetic moment parallel to the magnetically easy c-axis is forbidden by symmetry. The magnetic structure of CePdAl changes again at a second phase transition between 600 mK and 1.3 K. Future single-crystal neutron diffraction experiments must be awaited to reliably establish the low-temperature magnetic structure of CePdAl, which remains incommensurate down to 53 mK.

Table 5. A comparison of magnetic properties of the isostructural compounds TbNiAl and CePdAl with hexagonal ZrNiAl-type crystal structure (space group $P\bar{6}2m$ with magnetic atoms on site 3f): $T_{N,1}$, $T_{N,2}$, Néel temperatures; $\boldsymbol{k}_1, \boldsymbol{k}_2$, magnetic propagation vectors; Ln, Tb or Ce; μ_1, μ_2, ordered magnetic moments parallel to the c-axis.

	TbNiAl [3]	CePdAl this work
$T_{N,1}$ (K)	47	2.7
$T_{N,2}$ (K)	23	$0.6 < T_{N,2} < 1.3$
$\boldsymbol{k}_1$	$[1/2, 0, 1/2]$	$[1/2, 0, \tau]\tau \approx 0.35$
$\boldsymbol{k}_2$	$[0, 1/2, 1/2]$	$\boldsymbol{k}_2 \neq \boldsymbol{k}_1, \boldsymbol{k}_2 = ?$
$T_{N,2} < T < T_{N,1}$		
Ln(1)	$\boldsymbol{k}_1, \mu_1$	$\boldsymbol{k}_1, \mu_1$
Ln(2)	$\boldsymbol{k}_1, \mu_2$	disordered, μ_2
Ln(3)	$\boldsymbol{k}_1, \mu_1$	$\boldsymbol{k}_1, \mu_1$
	at 28 K	at 1.5 K
μ_1 (μ_B)	7.9 ± 0.2	1.58 ± 0.02
μ_2 (μ_B)	1.2 ± 0.3	0
$T < T_{N,2}$		
Ln(1)	$\boldsymbol{k}_1, \mu_1$	?
Ln(2)	$\boldsymbol{k}_2, \mu_2$	?
Ln(3)	$\boldsymbol{k}_1, \mu_1$	?
	at 2 K	at 0.6 K
μ_1 (μ_B)	8.7 ± 0.1	?
μ_2 (μ_B)	8.4 ± 0.3	?

Table 6. Magnetic modes calculated by the program MODY [10] for the case of space group $P\bar{6}2m$, site 3f and a commensurate propagation vector $\boldsymbol{k}_1 = [1/2, 0, 1/2]$.

			(0.58, 0, 0)			(0, 0.58, 0)			(0.42, 0.42, 0)		
			x	y	z	x	y	z	x	y	z
Representation τ_1 $(+,+,+,+)$											
$\boldsymbol{k}_1$	type 1	${}^1\phi^{1'}$	0	0	1				0	0	1
Representation τ_2 $(+,-,-,+)$											
$\boldsymbol{k}_1$	type 1	${}^1\phi^{2'}$	1	0	0				1	1	0
		${}^1\phi^{2''}$	0	1	0				0	−1	0
$\boldsymbol{k}_1$	type 2	${}^2\phi^{2'}$				0	1	0			
Representation τ_3 $(+,-,+,-)$											
$\boldsymbol{k}_1$	type 1	${}^1\phi^{3'}$	0	0	1				0	0	−1
$\boldsymbol{k}_1$	type 2	${}^2\phi^{3'}$				0	0	1			
Representation τ_4 $(+,+,-,-)$											
$\boldsymbol{k}_1$	type 1	${}^1\phi^{4'}$	1	0	0				−1	−1	0
		${}^1\phi^{4''}$	0	1	0				0	1	0
$\boldsymbol{k}_1$	type 2	${}^2\phi^{4'}$				1	0.5	0			

Acknowledgments

Financial support by the Swiss National Science Foundation and the Paul Scherrer Institute is gratefully acknowledged. For stimulating discussions concerning the use of the program MODY [10] we thank W Sikora.

References

[1] See, e.g., Bauer E 1991 *Adv. Phys.* **40** 417
[2] Maletta H and Sechovsky V 1994 *J. Alloys Compounds* **207/208** 254
[3] Ehlers G and Maletta H 1996 *Z. Phys.* B **99** 145
[4] Hulliger F 1993 *J. Alloys Compounds* **196** 225
[5] Schank C, Jährling F, Luo L, Grauel A, Wassilew C, Borth R, Olesch G, Bredl C D, Geibel C and Steglich F 1994 *J. Alloys Compounds* **207/208** 329
[6] Kitazawa H, Matsushita A, Matsumoto T and Suzuki T 1994 *Physica* B **199/200** 28
[7] Hulliger F 1995 *J. Alloys Compounds* **218** 44
[8] Dönni A, Kitazawa H, Fischer P, Tang J, Kohgi M, Endoh Y and Morii Y 1995 *J. Phys.: Condens. Matter* **7** 1663
[9] Tang J, Matsushita A, Kitazawa H and Matsumoto T 1996 *Physica* B **217** 97
[10] Sikora W 1994 *Workshop on Magnetic Structures and Phase Transitions (Krakow, 1994)* p 93
[11] Schefer J, Fischer P, Heer H, Isacson A, Koch M and Thut R 1990 *Nucl. Instrum. Methods* A **288** 477
[12] Rodriguez-Carvajal J 1993 *Physica* B **192** 55
[13] Sears V F 1992 *Neutron News* **3** 26
[14] Xue B, Schwer H and Hulliger F 1994 *Acta. Crystallogr.* C **50** 338
[15] Isikawa Y, Mizushima T, Fukushima N, Kuwai T, Sakurai J and Kitazawa H 1996 *J. Phys. Soc. Japan* (Suppl. B **65** 127)
[16] Ehlers G and Maletta H 1996 *Z. Phys.* B **101** 317